JOURNAL OF CATALYSIS 80, 263–273 (1983)

Catalytic Anisotropy of MoO_3 in Oxidation Reactions in the Light of Bond-Strength Model of Active Sites

JACEK ZIÓŁKOWSKI

Institute of Catalysis and Surface Chemistry, Polish Academy of Sciences, 30-239 Kraków, ul. Niezapominajek, Poland

Received February 5, 1982; revised August 3, 1982

Catalytic anisotropy of molybdic oxide in oxidation of propylene has been observed by Volta *et al.* (7th Int. Congr. Catal. Commun. C4, Tokyo, 1980; Faraday Disc. 72/13, Selectivity in Heterogeneous Catalysis, Nottingham, 1981). High selectivity to acrolein in the indicated reaction was ascribed to the (100) plane while the (010) plane was found to yield CO_2. The critical discussion of Volta's experimental data, performed in this paper, has shown that they may be interpreted in three alternative ways, differing in the ascription of the reaction products to the crystallographic planes. Different crystallographic planes exposed by the grains of MoO_3 have been analyzed in terms of the bond-strength model of active sites (Ziółkowski, *J. Catal.*, submitted) developed under the following main assumptions: (i) the reaction path depends on the number and configuration of the active oxygen atoms in the vicinity of the adsorption site, and (ii) the individual catalytic activity of a given surface oxygen atom is proportional to the reciprocal sum of the strength of the bonds to it from the adjacent cations. The analysis provided the arguments to indicate the most probable reaction pattern. According to it the main products expected to be formed in oxidation of propylene on different planes of MoO_3 are (100), CO, CO_2; (001), acrolein (acrylic acid, C_2–O, CO, CO_2—mainly at longer contact time); (101) and ($\bar{1}01$), acrolein; (010), inactive (possible minor yield of hexadiene and benzene).

INTRODUCTION

It has been found by Volta *et al.* (*1*, *2*) that the catalytic properties of molybdic oxide in the oxidation of propylene depend on the kind of crystallographic plane preferentially exposed by the grains of the polycrystalline sample. High selectivity to acrolein in the above-mentioned reaction was ascribed to the (100) plane while the (010) plane was found to yield CO_2. Ethanal and propanal were observed as minor reaction products, but no plane effect was discovered. A more profound analysis of Volta's experimental results performed in this paper indicates however that they may be interpreted in three alternative ways markedly differing in ascription of the reaction products to the kind of exposed crystallographic planes.

It will be shown in this paper that theoretical analysis performed in terms of the bond-strength model of active sites (*3*, *4*) provides the arguments to indicate the most probable reaction pattern of the three resulting from the experiments.

ANALYSIS OF EXPERIMENTAL DATA

Volta's MoO_3/graphite samples (labeled throughout this paper as I–V) were prepared from $MoCl_5$–graphite intercalation compounds by differentiated oxythermal treatment, during which MoO_3 crystals grew epitaxially on the graphite support. Their shapes, their dimensions, and consequently the contribution of various crystallographic planes in the external grain surface changed along the series, as determined by scanning and diffraction electron microscopy. MoO_3 grains were of hexagonal (I–IV) or rectangular (V) plate shape with the large face corresponding to the (010) plane, as shown in Fig. 1. Statistical determination of crystal lengths was done in [010], [001], [100] and equivalent [101] + [$\bar{1}$01] directions in different planes

0021-9517/83 $3.00

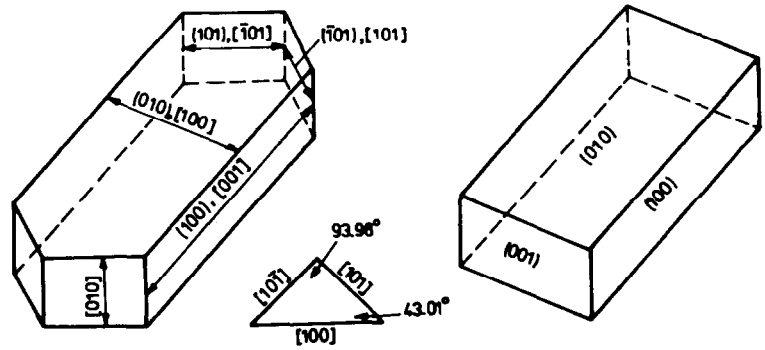

FIG. 1. Morphology of MoO_3 grains (*2*). In the center, relations are indicated between [100], [101], and [$\bar{1}$01] directions in MoO_3 structure.

and the respective data are given in Table 1. It should be stressed that, as the angles between [101], [$\bar{1}$01], and [100] result from the known lattice parameters of MoO_3 (*5*) (Fig. 1), one may easily calculate the crystal dimension along [101] + [$\bar{1}$01] knowing that along [100] and vice versa. The respective data are included in Table 1. The differences between the experimental and calculated lengths along [100] and [101] + [$\bar{1}$01], respectively (exceeding in the worse case 30%), illustrate the (unavoidable) experimental error of the applied method. This influences the accuracy of all further related calculations. In the present paper, to reach the most objective conclusions, three numbers are always given for the plane contribution (Table 2) and other data (Table 3). The first of them is taken from Volta's paper, the second is calculated from the crystal lengths—$[010]_{exp}$, (100) $[001]_{exp}$, (001) $[100]_{exp}$, (010) $[100]_{exp}$, and (101) ($\bar{1}$01) [$\bar{1}$01] $[101]_{calc}$, and the third from the three former, (101) ($\bar{1}$01) [$\bar{1}$01][101]$_{exp}$, and (010) $[100]_{calc}$.

Table 2 shows the initial selectivities S to acrolein and CO_2 (*2*) for all five samples under discussion, as well as the contribution (percentage) P of each crystallographic plane exposed by MoO_3 grains (Table 2A). Simple, qualitative inspection of Table 2 enables us to note the relation between S_{acr} and $P_{(100)}$ or S_{CO_2} and $P_{(010)}$, the first two increasing and the other two decreasing along the series. The respective correlations are better seen if—as proposed by Volta—the ratios $S_{acr}/P_{(100)}$ and $S_{CO_2}/P_{(010)}$ are taken into account, expressing as it were the initial selectivities per unit surface area (Table 3A). The numbers in each of the two sets are close to one another and the standard deviations from the average values are reasonably small. This leads to the conclusion, originally formulated by Volta,

TABLE I

Mean Length of MoO_3 Crystals in Different Planes and Directions

Sample	[010] exp	(100) [001] exp	(001) [100] exp	(010) [100] exp	(101) and ($\bar{1}$01) [$\bar{1}$01] + [101] exp	(010) [100] calc	(101) and ($\bar{1}$01) [$\bar{1}$01] + [101] calc
I	1	18	0	6	8	5.85	8.20
II	4	40	0	13	20	14.63	17.77
III	6	20	0	12	14	10.24	16.40
IV	2.5	9	0	6	6	4.38	8.20
V	1.5	5	3	3	0	3	0

TABLE 2

Initial Selectivities S to Acrolein and CO_2 and Contribution (Percentage) P of Different Crystallographic Planes Exposed by MoO_3 Crystals[a]

	Sample	I	II	III	IV	V	Trend
	S_{ACR}	24.2	32.8	42.0	41.6	52.0	↗
	S_{CO_2}	62.9	55.7	44.0	44.2	36.0	↘
A	$P_{(100)}$	10	16	18	18	28	
		12	19	23	20	28	↗
		12	17	26	26	28	
	$P_{(010)}$	85	76	61	64	55	
		83	72	58	62	55	↘
		82	74	55	56	55	
	$P_{(101)+(\bar{1}01)}$	5	8	21	18	0	
		5	9	19	18	0	↗
		5	9	18	18	0	
	$P_{(001)}$	0	0	0	0	17	
B	$P_{(100)}$	11	17	23	22	34	
		13	21	28	24	34	↗
		13	19	32	32	34	
	$P_{(010)}$	89	83	77	78	66	
		87	79	72	76	66	↘
		87	81	68	68	66	
C	$P_{(010)}$	85	76	61	64	55	
		83	72	58	62	55	↘
		82	74	55	56	55	
	$P_{(100)+(101)+(\bar{1}01)+(001)}$	15	24	39	36	45	
		17	28	42	38	45	↗
		17	26	44	43	45	
D	$P_{(010)}$	94	90	74	78	76	
		94	89	75	77	76	↘
		94	89	75	77	76	
	$P_{(101)+(\bar{1}01)+(001)}$	5	10	26	22	24	
		6	11	25	22	24	↗
		6	11	25	23	24	
E	$P_{(100)}$	66	66	46	50	(62)	
		68	69	55	52	(62)	↘
		69	67	58	60	(62)	
	$P_{(101)+(\bar{1}01)+(001)}$	33	33	54	50	(38)	
		32	31	45	48	(38)	↗
		31	33	42	40	(38)	

[a] Calculated at various assumptions, as explained in text.

that the (100) plane yields selectively acrolein and the (010) plane is responsible for combustion. Consequently it is understood that the (001), (101), and ($\bar{1}$01) planes are of negligible catalytic activity. If so, their contribution in the external grain surface should be omitted, as done in Tables 2B and 3B on the assumption that $P_{(100)} + P_{(010)} =$ 100%. The correlation is now, it is true, less accurate but it still exists.

The conclusion of the above discussion may be briefly summarized as follows:

A/B: (010), CO_2; (100), acrolein; (101), ($\bar{1}$01), (001), inactive.

More profound analysis of Table 2 makes

TABLE 3

S/P Ratios, Their Averages and Standard Deviations as a Measure of *S-P* Correlation

	Sample	I	II	III	IV	V	Average	σ	σ%
A	$\frac{S_{ACR}}{P_{(100)}}$	2.4	2.1	2.3	2.3	1.9			
		2.0	1.7	1.8	2.1	1.9	1.97	0.25	12
		2.0	1.9	1.6	1.6	1.9			
	$\frac{S_{CO_2}}{P_{(010)}}$	0.7	0.7	0.7	0.7	0.7			
		0.8	0.8	0.8	0.7	0.7	0.73	0.05	6
		0.8	0.8	0.8	0.8	0.8			
B	$\frac{S_{ACR}}{P_{(100)}}$	2.3	1.9	1.8	1.9	1.5			
		1.9	1.6	1.5	1.7	1.5	1.70	0.26	15
		1.9	1.7	1.3	1.3	1.5			
	$\frac{S_{CO_2}}{P_{(010)}}$	0.7	0.7	0.6	0.6	0.5			
		0.7	0.7	0.6	0.6	0.5	0.63	0.07	10
		0.7	0.7	0.6	0.6	0.5			
C	$\frac{S_{ACR}}{P_{(101)} + (\bar{1}01) + (100) + (001)}$	1.6	1.4	1.1	1.2	1.2			
		1.4	1.2	1.0	1.1	1.2	1.19	0.18	14
		1.4	1.3	1.0	1.0	1.2			
	$\frac{S_{CO_2}}{P_{(010)}}$	0.7	0.7	0.7	0.7	0.7			
		0.8	0.8	0.8	0.7	0.7	0.73	0.05	6
		0.8	0.8	0.8	0.8	0.7			
D	$\frac{S_{ACR}}{P_{(101)} + (\bar{1}01) + (001)}$	4.4	3.4	1.6	1.9	2.2			
		4.3	2.9	1.6	1.8	2.2	2.63	0.98	37
		4.2	3.0	1.7	1.8	2.2			
	$\frac{S_{CO_2}}{P_{(010)}}$	0.7	0.6	0.6	0.6	0.5			
		0.7	0.6	0.6	0.6	0.5	0.58	0.06	11
		0.7	0.6	0.6	0.6	0.5			
E	$\frac{S_{ACR}}{P_{(101)} + (\bar{1}01) + (001)}$	0.7	1.0	0.7	0.8	(1.4)			
		0.8	1.0	0.9	0.8	(1.4)	0.90	0.11	12
		0.8	1.0	1.0	1.0	(1.4)			
	$\frac{S_{CO_2}}{P_{(100)}}$	1.0	0.8	1.0	0.9	(0.6)			
		0.9	0.8	0.8	0.9	(0.6)	0.86	0.07	8
		0.9	0.8	0.8	0.7	(0.6)			

it possible, however, to indicate three other possible correlations corresponding to the following catalytic features:

C: (010), CO_2; (100), (101), ($\bar{1}$01), (001), acrolein

D: (010), CO_2; (101), ($\bar{1}$01), (001), acrolein; (100), inactive

E: (010), inactive; (101), ($\bar{1}$01), (001), acrolein; (100), CO_2.

The contribution *P* and the ratios *S/P* for the respective planes corresponding to C, D, and E, calculated in the same manner as explained above, are shown in Tables 2 and 3 (rows C, D, and E, respectively). As indicated from Table 3 there is no quantitative correlation for D, while C and E give correlations as good as A/B or even better if compared with B. In the last case (E) a good correlation was found if the results for sample V were omitted. To explain this fact it should be recalled that samples I–IV on the one hand and sample V on the other differ in shape, the first four exposing equivalent (101) + ($\bar{1}$01) planes and the last one the (001) plane. It seems obvious that the ratio *S/P* for a given product and a given plane (given site) depends not only on the

preferred formation of this product but also on the reaction rate. Thus the *S/P* ratio for a given product and different planes (different sites) are not necessarily the same.

In the light of Volta's paper and the above discussion, the catalytic anisotropy of MoO_3 seems to be well argued, but the question of which planes are responsible for selective formation of acrolein and CO_2 remains open. Of three possible answers two (A/B and C) are very similar but the third (E) is exactly opposite.

BOND-STRENGTH MODEL OF ACTIVE SITES

Another example of catalytic anisotropy has been observed recently in our laboratory during studies on the oxidation of propylene (*6*) and *o*-xylene (*4*) over $Mn_{1-x}\phi_xV_{2-2x}Mo_{2x}O_6$ (further denoted as MV-X, X = 100*x*) solid solutions of the brannerite-type structure (*7*). To explain the different catalytic properties of the (201) and (20$\bar{2}$) planes of MV-X a new model of sites active in hydrocarbon oxidation reactions has been developed (*3, 4*) based on the assumptions which are formulated below.

1. The first, activating step of oxidation of propylene (as for other molecules cf. point 5) lies in its dissociative adsorption with abstraction of α-hydrogen and formation of π-allylic intermediate. For this purpose two kinds of centers are required at the surface: (i) the oxidative dehydrogenation centers (as for Mo-containing oxide catalysts, Mo=O groups were proposed as such centers (*8–13*)) and (ii) the adsorption sites consisting of coordinately unsaturated metal atoms with empty orbitals of low energy, ensuring some shift of electrons to the catalyst (*14–16*). Symmetrical π-allyl is adsorbed in the plane parallel to the catalyst surface and its orientation depends on the symmetry of the local crystal field (*17*). The abstracted hydrogen atoms forming –OH groups may move along the surface combining finally with surface oxygens to form molecules of water.

2. The further transformations of allyl depend on the number and configuration of active oxygen atoms around the adsorption site. These factors determine if one or more oxygen atoms may be incorporated on one site. If one, acrolein is primarily expected as the reaction product; more oxidized products may be eventually formed in the consecutive reactions after readsorption on the other site and the selectivity may be ruled by changing the contact time. If more than one (and conveniently arranged), the reaction selectivity depends on the probability of desorption of various products formed on one site and it is much less dependent on external reaction conditions.

3. The structure (configuration, bond length) at the surface is assumed to be the same as in the bulk as known from the crystallographic data for the given catalyst. The crystal is "cut" in such a manner as to retain the stoichiometric composition. Oxygen atoms completing the respective polyhedra are regarded as adsorbed atoms. Usually only a part of these sites is occupied.

4. The individual activities of surface oxygen atoms are assumed to be proportional to the reciprocal sums of the strength of the bonds to them (ΣS_i) from the adjacent cations. The latter are calculated according to the bond-length–bond-strength concept using the most recent formula and data (*18*) (cf. Appendix). Three types of surface oxygen atoms may be distinguished:

(a) firmly bound inactive lattice oxygen atoms O_{IL} of $\Sigma S_i \approx 2$,

(b) loosely bound active lattice oxygen atoms O_{AL} of $\Sigma S_i < 1.85$, and

(c) loosely bound active adsorbed oxygen atoms O_{AA} of ΣS_i usually smaller then 1.

5. It is believed that the model, successfully explaining the oxidation of propylene on MV-X (*3*), may also be applied to other catalysts and to oxidation of other organic molecules provided that assumption 1 is replaced by the respective data concerning their adsorption. The first step in such a generalization of the model has been already made (*4*) (oxidation of *o*-xylene over MV-X).

It seems of interest to apply the above-

sketched model to the oxidation of propylene on the different planes of MoO_3 crystals.

CONSIDERATION OF MoO_3 SURFACE STRUCTURE IN THE LIGHT OF THE BOND-STRENGTH MODEL OF ACTIVE SITES

i. Structure of MoO_3

MoO_3 crystallizes in the orthorhombic system, $a = 3.9628$ Å, $b = 13.855$ Å, $c = 3.6964$ Å, the space group is *Pbnm* (*5*). As shown in Fig. 2 this is a layer structure in which each layer is built up of MoO_6 octahedra at two levels, connected along c by common edges and corners so as to form zig-zag rows and along a by common corners only. In the idealized presentation (regular octahedra) each next layer is simply shifted by $\frac{1}{2}(a + b)$. In fact, the octahedra are markedly disturbed (Mo–O distances vary between 1.671 and 2.332 Å) and the deformations along a are opposite in the neighboring layers. The exact respective values of Mo–O distances (*5*) have been used to calculate S_i and ΣS_i as proposed by Brown and Kang Kun Wu (*18*) (cf. Appendix).

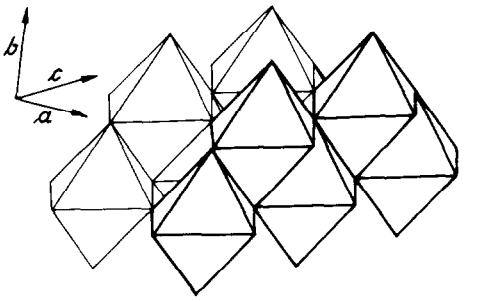

FIG. 2. Idealized presentation of a part of one layer in MoO_3 structure (after Kihlborg (*5*)).

ii. (010) Plane

Figure 3 shows the arrangement of atoms

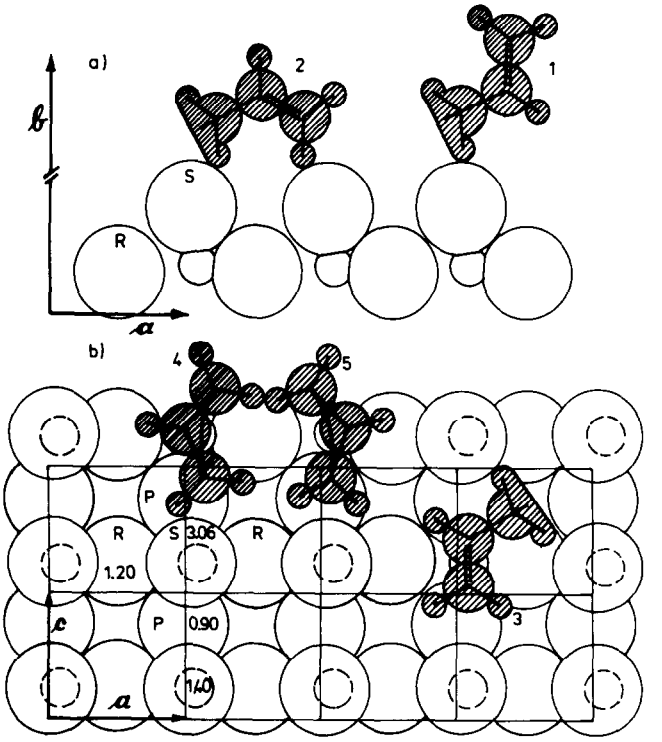

FIG. 3. (010) plane of MoO_3 (b) and its side view (a) with: (1,2) propylene adsorbed through the hydrogen bonds, (3) π-adsorbed propylene, and (4,5) π-allyls adsorbed in configuration enabling formation of hexadiene. For Figs. 3–6: large circles, oxygen; small circles, molybdenum; double circles, active oxygen atoms; double dotted circles, adsorbed oxygen atoms. Capital letters distinguish the structurally different oxygen atoms. The numbers indicate the distances of atoms from the plane.

on the (010) plane. It consists of corner-sharing square pyramids built of three structurally different atoms: two O_P (1.90), two O_R(1.98), and one O_S(2.04). The respective values of ΣS_i given in parantheses indicate that all of them are catalytically inactive in terms of the bond-strength model of active sites. Adsorption of propylene on metal atoms is impossible as they are covered by O_S atoms.

The completely oxidized (010) plane should thus be catalytically inactive in oxidation. The only possibility of adsorptive interaction between propylene and the oxidized (010) plane of MoO_3 seems to consist in the formation of one or two hydrogen bridges, as shown in Fig. 3a. As firmly bound O_S (belonging to the Mo=O group) participates in the hydrogen bonding, oxidative dehydrogenation seems to be possible, resulting in formation of $-CH_2-CH-CH_2$, $-CH-CH-CH_2$, $-CH_2-CH-CH-$, or similar σ-bonded intermediates. If formed on the adjacent O_S sites these intermediates might combine to yield hexadiene or benzene, provided that desorption of water is possible from the (010) plane or that hydrogen atoms may diffuse toward other planes rich in loosely bound oxygen.

If the (010) plane were slightly reduced, some O_S positions would be empty and propylene might form a π-allylic intermediate (or other deeply dehydrogenated, π-bonded species) (Fig. 3b). The expected distribution of products in such a case is, however, the same as discussed above, as there is no active oxygen around the adsorption site which could be inserted.

To simplify further discussion concerning other planes of MoO_3 let us mention here that on each of them oxidative dehydrogenation centers (Mo=O) are present. These are O_B and O_C on the (100) plane, O_L on the (001) plane, and O_Z on the (101) plane (cf. Table 6). Moreover, noncovered Mo atoms exist on all those planes. α-Hydrogen abstraction may thus proceed there both (i) through the intermediate linked to the surface with the hydrogen bond and (ii) through π-bonded propylene as intermediate. In the later case the above mentioned process should be easier than in the former, due to the positive charge which appears on

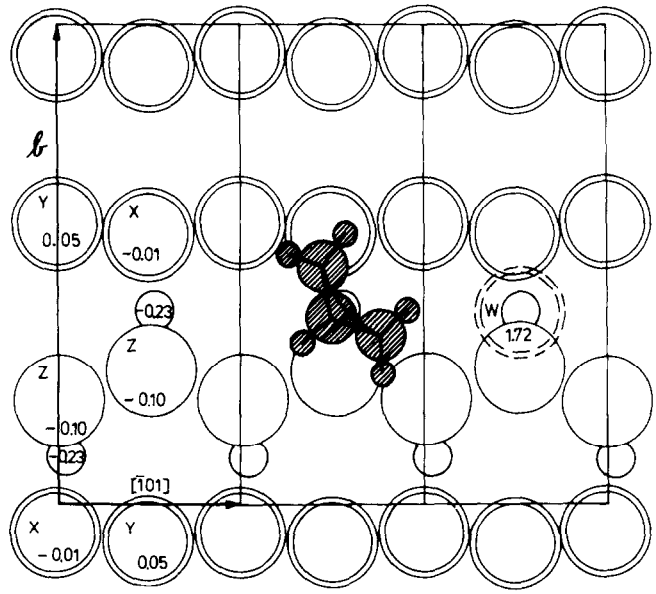

FIG. 4. (101) or equivalent (101) plane of MoO_3 (origin shifted by z = 0.92 Å) with adsorbed π-allyl (cf. Fig. 3).

propylene after π-type adsorption (*14–16*). This may serve as an argument for higher activity of all discussed planes as compared to (010).

iii. Equivalent (101) and ($\bar{1}01$) Planes

Along the (101)/($\bar{1}01$) planes (Fig. 4) two oxygen atoms are lacking in each MoO_6 group, the coordination of molybdenum becoming tetrahedral. Each Mo atom is linked with $O_X(1.09)$ and $O_Z(2.04)$ in the plane and with two other oxygen atoms in the bulk. These tetrahedra form the zig-zag rows. Between them $O_Y(1.63)$ atoms appear, being the apices of MoO_6 groups localized below the surface. The fourth oxygen O_W of estimated $\Sigma S_i \approx 0.8$ may be adsorbed over the Mo position. On the same site a π-allylic intermediate may be formed, which in turn may incorporate one atom of active oxygen O_X to form acrolein. The expected selectivity to acrolein is very high (at least for shorter contact time) since there is no more active oxygen atom in the nearest vicinity of the adsorption site. At most O_Y adjacent to O_X could probably be inserted yielding acrylic acid. Other O_X and O_Y and adsorbed O_W are very distant. More oxidized product could thus appear exclusively on the condition that adsorption reiterates. However, even in such a case the geometry of the plane makes possible the interactions of active surface oxygen atoms only with lateral carbons of the π-bonded C_3 molecule and never with the C–C bond. Degradation of the C_3 branch and total combustion thus seem impossible.

It seems of interest to mention that the loosely bound lattice O_X and O_Y atoms form the rows in the (101)/($\bar{1}01$) planes along which easy surface diffusion might proceed providing oxygen atoms required for the reformation of the exhausted active sites.

iv. (001) Plane

The arrangement of atoms on the (001) plane is presented in Fig. 5. This plane is built of parallel rows of corner-sharing squares formed of two $O_K(1.98)$, one $O_L(2.04)$, and one $O_M(1.09)$ with molybdenum atoms inside. All five atoms lie on exactly the same plane. The other oxygen $O_N(0.81)$ may be adsorbed over the Mo position. Similarly to the (101) plane on the same site a π-allylic intermediate may be formed, which in turn may incorporate one

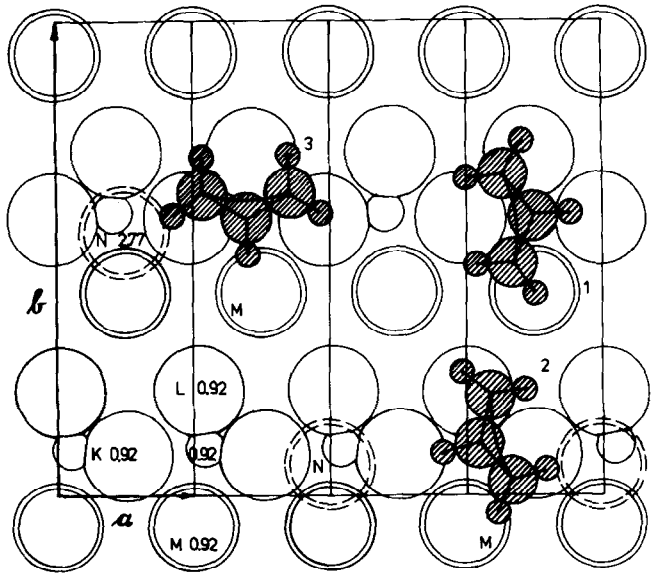

FIG. 5. (001) plane of MoO_3 with π-allyl adsorbed in three different situations (1,2,3) (cf. Fig. 3).

atom of active oxygen O_M to form acrolein (Fig. 5, situation 1). Some part of π-allyls or preformed acrolein may undergo further oxidation to acrylic acid (Fig. 5, situation 2) or C_2–O product (Fig. 5, situation 3) already on the same center, if the adjacent Mo site is covered with O_N. As the adsorbed propylene may be attacked on one center at most by two active oxygen atoms initial selectivity to the total combustion products is expected to be nought. In contrast, in the case of readsorption all products of deeper oxidation may appear. Acrolein is thus the main reaction product expected for the (001) plane, formed however with selectivity inferior to that for the (101) plane and decreasing with increasing contact time.

V. (100) Plane

The structure of the (100) plane (Fig. 6) is a bit more complex. It is composed of the parallel zig-zag rows of edge-sharing squares formed of three O_A(1.90) and one O_B(2.04) or one O_C(2.04) with Mo atoms inside. These Mo-containing rows are separated by two other rows of O_D(0.34) and O_E(1.63). The above-mentioned atoms together form the stoichiometric and flat (100) plane. There are two different positions above the plane for oxygen atoms completing the respective octahedra, namely, O_F(0.34) and O_G(1.63). Due to the great difference in the bond strength of O_G and O_D it seems more reasonable to assume that the (100) plane is actually composed of O_A, O_B, O_C, O_E, and O_G (all quoted positions being completely filled up) and to consider O_D and O_F as adsorption sites, which in part may be occupied by oxygen. At the same sites, similar to the previously discussed planes, propylene may be adsorbed. As seen in Fig. 6 each adsorption site in the (100) plane is surrounded by two active lat-

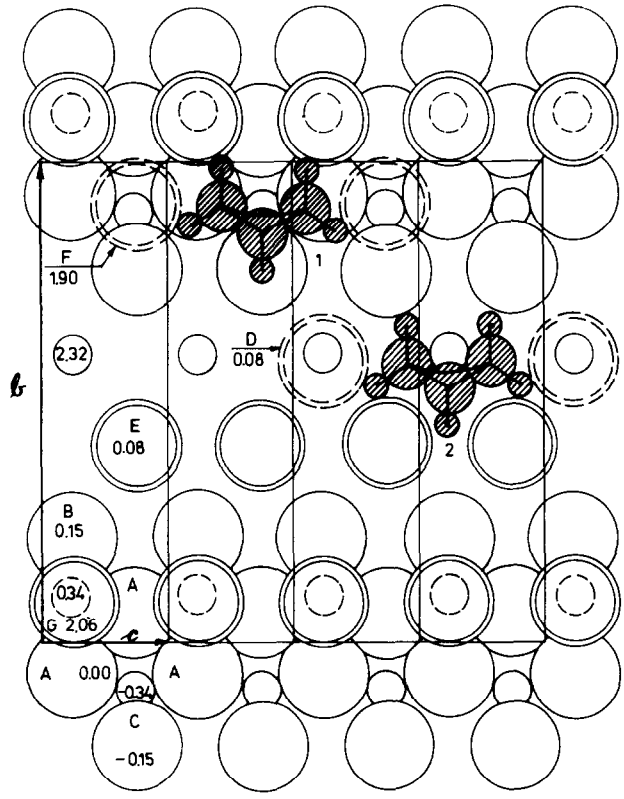

FIG. 6. (100) plane of MoO_3 with π-allyl adsorbed in two different situations (1,2) (cf. Fig. 3).

tice oxygen atoms (O_G or O_E) and frequently in addition by one or two active adsorbed oxygen atoms (O_D or O_F). The probability of the selective oxidation of propylene should thus be diminished in favor of degradation and total combustion.

CONCLUSIONS

The theoretical considerations presented in the preceding section of the paper, based on the bond-strength model of active sites, clearly demonstrate that the population and structure of sites active in conversion of propylene on MoO_3 are very differentiated if various crystallographic planes are taken into account. All discussed planes, i.e. (010), (101), (100), and (001), are endowed with oxidative dehydrogenation centers (Mo=O groups) on which hydrogen abstraction may take place through hydrogen-bonded or through π-bonded intermediates (the latter being impossible on the completely oxidized (010) plane). As active oxygen atoms are absent on the (010) plane hexadiene and benzene are the only expected products yielded on this plane. In contrast, a variety of active oxygens may be indicated on the other planes. Sometimes—as for the (101) plane—they are isolated, which favors the selective formation of acrolein. Sometimes they form groups around the adsorption Mo-site, which gives rise to a yield of more oxidized products. Further differentiation of the reaction pattern is expected when adsorption may reiterate (longer contact time). The final conclusion concerning the product distribution on different crystallographic planes is presented in Table 4. As seen, it is close to one of three possible patterns resulting from experiments and referred to as E under Analysis of Experimental Data.

TABLE 4

The Main Products Formed on Different Crystallographic Planes of MoO_3 in Oxidation of Propylene, as Results from the Analysis Performed in Terms of the Bond-Strength Model of Active Sites

Plane	Products
(010)	Inactive or (hexadiene)[a] (benzene)[a]
(101), ($\bar{1}$01)	Acrolein (acrylic acid)[a]
(001)	Acrolein (acrylic acid)[b] (C_2–O)[b] (combustion)[b]
(100)	Combustion

[a] Minor products.
[b] Products expected mainly at longer contact time.

Some products indicated in Table 4 (hexadiene, benzene, acrylic acid) have never been observed experimentally during oxidation of propylene on MoO_3. This may be due to the generally low activity of MoO_3 (low conversion) which is ascribed to the low surface area of usually used samples and to the difficult abstraction of the first hydrogen. If this difficulty was overcome by using allyl iodide (*19*), remarkable yields of acrolein and acrylic acid were observed and simultaneously hexadiene and benzene appeared in small quantities.

Quite recently Tatibouët and Germain (*13*) have provided a new example of the catalytic anisotropy of MoO_3 in the conversion of methanol. Analysis of these data in terms of the bond-strength model of active sites will be the subject of a forthcoming paper.

APPENDIX

According to Brown and Kang Kun Wu (*18*) cation-oxygen bond length (R) and its bond strength (S) are related by the equation

$$S = \left(\frac{R}{R_1}\right)^{-N} \qquad (1)$$

where R_1 and N are empirical parameters. For Mo^{6+}, $R = 1.882$, $N = 6$ (*18*).

TABLE 5

Lengths and Strengths of Mo–O Bonds in MoO_3

Bond	Length	Strength
Mo–O_3 (a)	1.734	1.635
Mo–O_4 (b)	1.671	2.041
Mo–O_2 (c)	2.332	0.276
Mo–O_3' (d)	2.251	0.342
2x Mo–O_2' (e)	1.948	0.813

TABLE 6

ΣS_i for All Surface Oxygen Atoms Discussed in this Paper[a]

Oxygen	Bonds	ΣS_i	Oxygen	Bonds	ΣS_i
(100) plane			(001) plane		
O_A	e, e, c	1.90	O_K	a, d	1.98
O_B	b	2.04	O_L	b	2.04
O_C	b	2.04	O_M	c, e	1.09
O_D	d	0.34	O_N	e	0.81
O_E	a	1.63			
O_F	d	0.34	(010) plane		
O_G	a	1.63	O_P	e, e, c	1.90
			O_R	a, d	1.98
			O_S	b	2.04
(101) or ($\bar{1}$01) plane					
O_X	c, e	1.09	O_Z	b	2.04
O_Y	a	1.63	O_W	Estimated	0.8

[a] Cf. Figs. 3–6.

Mo–O bond length in MoO_6 octahedra of MoO_3 (*5*) together with their bond strength calculated with Eq. (1) are gathered in Table 5. Table 6 summarizes the ΣS_i values for all surface oxygen atoms discussed in this paper. As the Mo–O bonds are indexed with the letters a–e the coordination of each surface oxygen may be easily recognized.

REFERENCES

1. Volta, J-C., Desquesnes, W., Moraweck, B., and Tatibouët, M. J., 7th Intern. Congr. Catal. Commun. C4, Tokyo, 1980.
2. Volta, J-C., Forissier, M., Theobald, F., and Pham, T. P., Faraday Disc. 72/13, Selectivity in Heterogeneous Catalysis, Nottingham, 1981.
3. Ziółkowski, J., *J. Catal.*, submitted May 15, 1981.
4. Ziółkowski, J., and Gąsior, M., *J. Catal.*, submitted May 27, 1982.
5. Kihlborg, L., *Arkiv Kemi* **21,** 357 (1963).
6. Ziólkowski, J., and Janas, J., *J. Catal.*, submitted January 21, 1981.
7. Kozłowski, R., Ziółkowski, J., Mocała, K., and Haber, J., *J. Solid State Chem.* **35,** 1 (1980), erratum **38,** 138 (1981).
8. Trifiro, F., and Pasquon, I., *J. Catal.* **14,** 412 (1968).
9. Trifiro, F., Centola, P., Pasquon, I., and Jiru, P., Proc 4th Intern. Congr. Catal., Moscow 1968, p. 310. Nauka, 1970.
10. Mitchell, P. C. H., and Trifiro, F., *J. Chem. Soc. A* 3183 (1970).
11. Trifiro, F., Notarbartolo, S., and Pasquon, I., *J. Catal.* **22,** 324 (1971).
12. Weiss, F., Marion, J., Metzger, J., and Cognon, J-M., *Kinet. Katal.* **14,** 45 (1973).
13. Tatibouët, J. M., and Germain, J. E., *J. Catal.* **72,** 375 (1981).
14. Haber, J., Sochacka, M., Grzybowska, B., and Gołębiewski, A., *J. Mol. Catal.* **1,** 35 (1975/76).
15. Haber, J., and Witko, M., *J. Mol. Catal.* **9,** 399 (1980).
16. Haber, J., and Witko, M., *Acc. Chem. Res.* **14,** 1 (1981).
17. Dadyburjor, D. B., Jewur, S. S., and Ruckenstein, E., *Catal. Rev. Sci. Eng.* **19,** 283 (1979).
18. Brown, I. D., and Kang Kun Wu, *Acta Crystallogr.* **B32,** 1957 (1976).
19. Grzybowska, B., Haber, J., and Janas, J., *J. Catal.* **49,** 150 (1977).